

Effects of rare earth Ce on properties of Sn–9Zn lead-free solder

WenXue Chen · Songbai Xue · Hui Wang ·
YuHua Hu · Jianxin Wang

Received: 8 July 2009 / Accepted: 23 September 2009 / Published online: 6 October 2009
© Springer Science+Business Media, LLC 2009

Abstract The influences of different Ce content on the properties of Sn–9Zn lead-free solder were investigated. The results indicate that Ce plays an important role not only in the structure and the solderability, but also in the interfacial structure of Sn–9Zn– x Ce/Cu and mechanical property of soldered joint. Sn–9Zn–0.08Ce shows finer and more uniform microstructure than Sn–9Zn, and when the quantity of Ce is 0.5–1 wt%, some dark Sn–Ce compounds appear in the solder. With the addition of 0.08 wt% Ce, the solderability of solder is significantly improved because the surface tension of molten solder is decreased. Adding Ce makes the Cu₅Zn₈ IMCs formed at the interface of solder/Cu become much thicker than that of Sn–9Zn/Cu because much more content of Zn diffuse to the interface of solder/Cu to react with Cu. Results also indicate that adding 0.08 wt% Ce to the solder enhances mechanical property of soldered joint. When the Ce content is 0.1–0.5 wt%, some hard and brittle Cu–Zn IMCs appear in the bottom of dimples and the pull force of soldered joint decreases.

1 Introduction

Sn–Pb alloys are widely used in electronics manufacturing because of their excellent properties and low cost. But

Pb and Pb-containing compounds are harmful to environment and human health. Due to marketing and legislative pressures, the electronics industries are moving to adoption of lead-free solders. So the research on Pb-free solders to replace Sn–Pb solder has become very important [1–6].

So far, the most widely researched lead-free solders include Sn–Ag, Sn–Cu, Sn–Bi, Sn–Zn binary alloys and Sn–Ag–Cu, Sn–Ag–Bi, Sn–Zn–Bi, Sn–Zn–Ag ternary alloys [3]. Among these lead-free solders, Sn–Zn solder is widely recommended because of its low melting point (198 °C, near that of the Sn–Pb alloy—183 °C), excellent mechanical properties and low cost. However, Sn–Zn solder suffers from easy oxidation and relatively poor wettability. Generally, there are two methods to partially improve wettability of Sn–Zn solder: one is to develop a new kind of flux which is fit for lead-free soldering; another is to improve oxidation resistance by alloying [7]. In this paper, we focus on the second one. Mao and coworkers [7] have reported that Cr addition can enhance the wettability because the addition of Cr increases the oxidation resistance of Sn–9Zn solder. Lin and coworker [8] have reported the effect of alloying addition of Al and Ga to Sn–Zn solder on oxidation resistance and wettability. Due to the unique properties of rare earth (RE) elements, some researchers have tried to improve the properties of Sn–9Zn solder by adding RE elements [9, 10]. But they focused on the mixed RE elements (Ce and La), and the studies on single rare earth adding to the Sn–9Zn solder are scarce. In this paper, the effects of rare earth Ce on microstructures, wettability of solder and the mechanical properties of soldered joints were studied, respectively, and the interfacial structure of Sn–9Zn– x Ce/Cu were also studied.

W. Chen · S. Xue (✉) · H. Wang · Y. Hu
Nanjing University of Aeronautics and Astronautics, Nanjing,
China
e-mail: xuesb@nuaa.edu.cn

J. Wang
Jiangsu University of Science and Technology, Zhenjiang, China

2 Experiment

2.1 Materials

Sn–9Zn– x Ce alloys with $x = 0, 0.03, 0.05, 0.08, 0.1, 0.5$, respectively, were prepared from 99.95% pure Sn, 99.999% pure Zn and 99.9% pure Ce. Under nitrogen atmosphere, the alloys were melted within quartz tubes, by homogenizing and repeatedly shaking at 500 °C over 3 h. During this process, KCl/LiCl eutectic mixture served as a barrier layer for oxidation. The compositions of alloys were investigated by inductively coupled plasma emission spectrometer (ICP-AES). The chemical compositions of the alloys used in this study are listed in Table 1.

2.2 Solderability test

According to Japanese industry standard JIS Z 3198-4 (Test methods for lead-free solders—Part 4: Methods for solderability test by a wetting balance method and a contact angle method), solderability of lead-free solders was assessed using wetting balance method with SAT-5100 Solder Checker. As shown in Fig. 1, the relationship between wetting force and time was recorded as the wetting curve. The test Cu foils (30 mm × 5 mm × 0.3 mm) were degreased in acetone for 1 min, ultrasonically cleaned in ethanol, and dried. These foils were coated with a no-clean flux before they were tested in the solderability tester. During the solderability test, the immersion depth and time

Table 1 Chemical compositions of solders (wt%)

Alloys	Zn	Ce	Sn
Sn–9Zn	8.761	0	Remainder
Sn–9Zn–0.03 Ce	8.780	0.031	Remainder
Sn–9Zn–0.05 Ce	8.893	0.048	Remainder
Sn–9Zn–0.08 Ce	8.786	0.082	Remainder
Sn–9Zn–0.1 Ce	8.804	0.096	Remainder
Sn–9Zn–0.5 Ce	8.785	0.512	Remainder

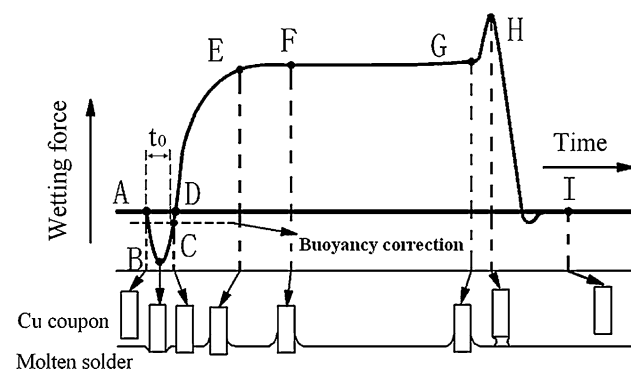


Fig. 1 The wetting curve of solder

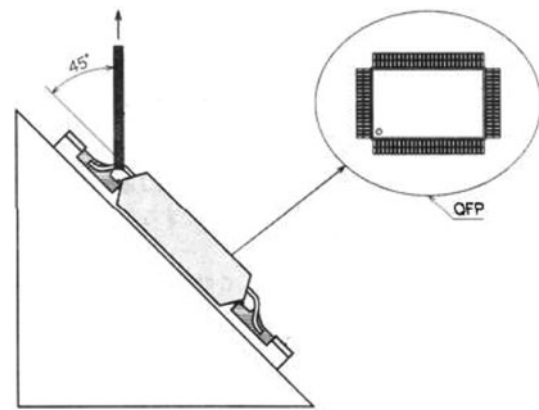


Fig. 2 Schematic diagram of micro joints strength test

were 2 mm and 10 s, respectively. The immersion speed was 5 mm s⁻¹. The soldering temperature of Sn–9Zn– x Ce alloys was 245 °C. Solderability test was carried out in air.

2.3 Mechanical property test

In order to reflect the actual instances in electronic assembly industry, quad flat packages (QFP) were soldered on PCB (Cu pad) using Sn–9Zn– x Ce solders. According to Japanese Industry Standard JIS Z 3198-6 (Test methods for lead-free solders—Part 6: Methods for 45 degree pull test of solder joints on QFP lead), the pull forces of the soldered joints were tested at room temperature with a STR-1000 joint strength tester, as schematically shown in Fig. 2.

3 Results and discussion

3.1 Microstructure of solder

Figure 3a–f shows the microstructures of Sn–9Zn, Sn–9Zn–0.03Ce, Sn–9Zn–0.05Ce, Sn–9Zn–0.08Ce, Sn–9Zn–0.1Ce, Sn–9Zn–0.5Ce alloys, respectively, under slow cooling. The Sn–9Zn eutectic alloy consists of two phases, namely, the β -Sn and Zn-rich phases with less than 1% Sn. The Zn was etched so that dark grooves were formed at the originally Zn-occupying sites. The rod like Zn-rich phase was formed during solidification because of the conglomeration of small Zn-rich phase. With the addition of 0.03–0.08% Ce to the Sn–9Zn alloy, the volume fraction and size of the needle-like phase decrease. As shown in Fig. 3d, a uniform and fine structure is obtained. In Fig. 3e, when the content of Ce is 0.1%, some dark particulate-shaped phases can be observed in the Sn-rich matrix. These dark phases are determined as the Sn–Ce intermetallic compounds by EDX analysis as shown in Fig. 4. Although Sn and Zn can form an intermetallic compound with Ce individually, the reaction temperature for Sn–Ce is under

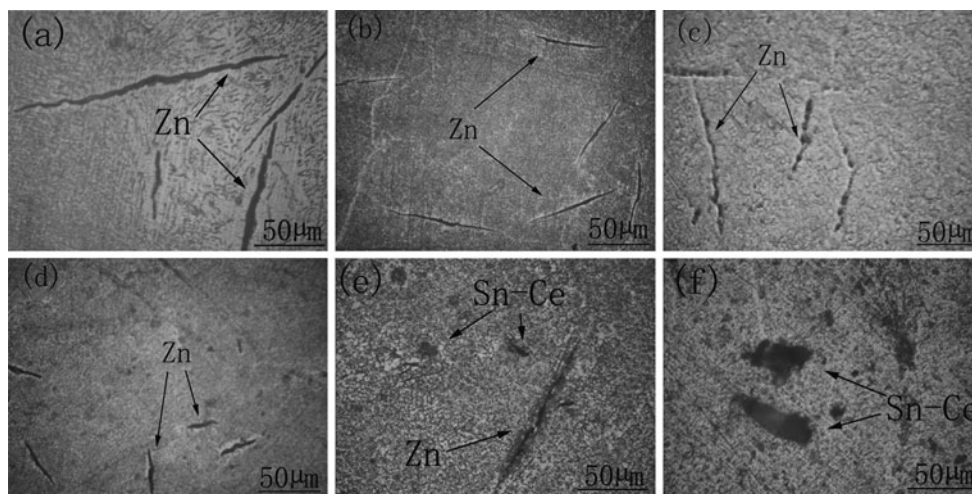


Fig. 3 OM micrograph of **a** Sn-9Zn, **b** Sn-9Zn-0.03Ce, **c** Sn-9Zn-0.05Ce, **d** Sn-9Zn-0.08Ce, **e** Sn-9Zn-0.1Ce, **f** Sn-9Zn-0.5Ce

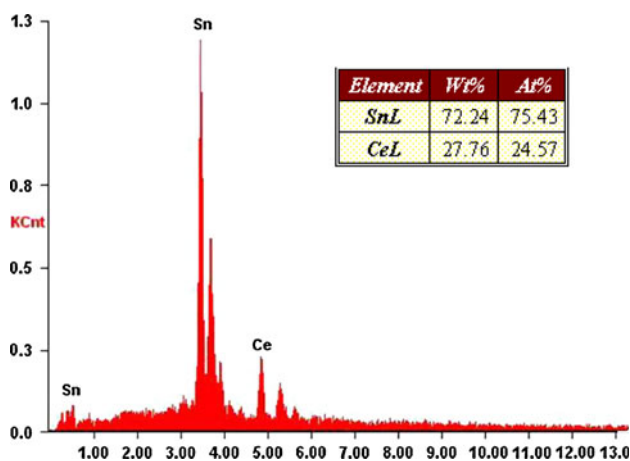


Fig. 4 EDS analysis of the dark phase

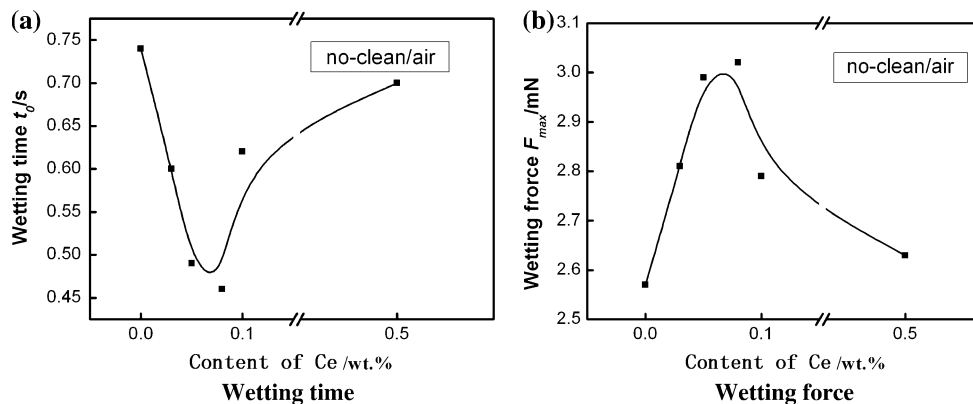
300 °C, while the temperature for Zn–Ce is nearly 500 °C [11]. The standard Gibbs free energy of formation for Sn–Ce is much lower than that of the Zn–Ce compound [12]. Hence, there is a tendency to form Sn–Ce compounds under the slow cooling. As the Ce content increases to

0.5%, the volume fraction of the Sn–Ce particles further increases, as shown in Fig. 3f.

3.2 Solderability of solder

Figure 5 shows the wetting properties (wetting time and wetting force) of Sn-9Zn-xCe lead-free solders at the temperature of 245 °C in air with no-clean flux. The solderability of solder on Cu substrate tends to be improved, namely, the wetting time is reduced and the wetting force is increased, when the Ce content is 0.03–0.08 wt%. The Sn-9Zn-0.08Ce solder has the smallest wetting time and biggest wetting force among these alloys. As an active element, Ce tends to accumulate at the solder interface in the molten state, thus the surface tension of molten solder is decreased effectively [13], which plays an important role in the improvement of the solderability. However, adding more than 0.1 wt% Ce into the solder appears to lower the solderability of the solder when compared with 0.08 wt% Ce alloy for the increase in solder viscosity. Because both Zn and Ce are easily oxidized during soldering, an increase

Fig. 5 Wetting properties of Sn-9Zn-xCe solders



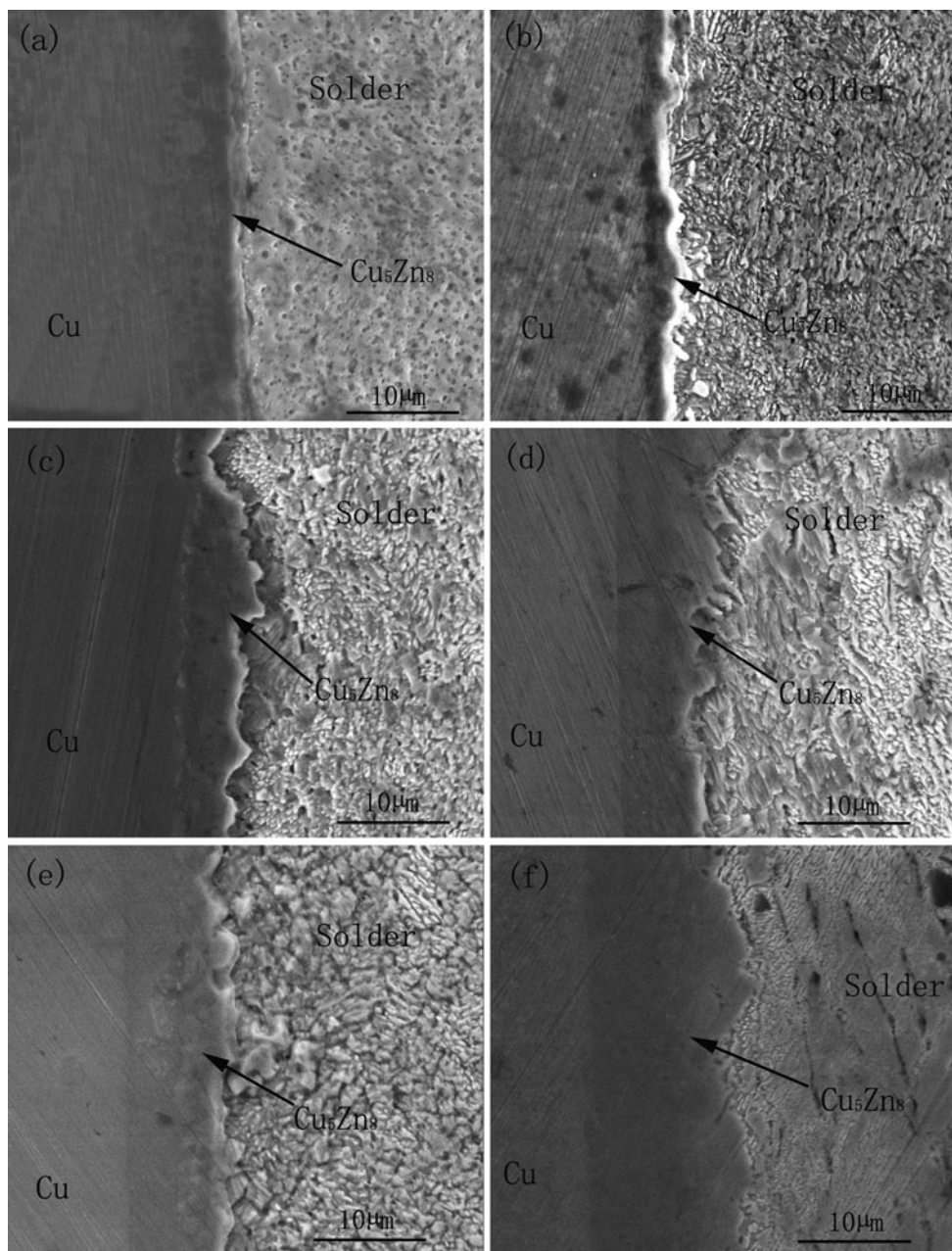


Fig. 6 Interfacial structure of **a** Sn-9Zn/Cu, **b** Sn-9Zn-0.03Ce/Cu, **c** Sn-9Zn-0.05Ce/Cu, **d** Sn-9Zn-0.08Ce/Cu, **e** Sn-9Zn-0.1Ce/Cu, **f** Sn-9Zn-0.5Ce/Cu

in the amount of Ce means an increase in the amount of oxides and inhibits the wetting behavior.

3.3 Interfacial structure of Sn-9Zn-*x*Ce/Cu

Figure 6 displays the cross-sectional morphologies of the Sn-Zn-*x*Ce/Cu interfaces. As shown in Fig. 6a, intermetallic compound formed at the Sn-Zn/Cu interface is a planar layer (Cu_5Zn_8). A Zn depletion zone can be observed in the vicinity of this interface. As shown in Fig. 7, on the surface of Sn-9Zn/Cu, the morphology of the

Cu_5Zn_8 compounds appears to have a granular appearance. No Cu-Sn phases are observed. The absence of the Cu-Sn phases may be due to two reasons. The first one is the limit of higher activation energy barrier of nucleation, which makes the Cu-Sn phases difficult to form. Second, these phases may form but have a relatively slow growth rate, which makes them too thin to be observed. This is similar to the result of the study by Chen et al. [14].

Before soldering, the Cu foils are coated with the flux to remove oxide layer of the surface, thus a number of temporary active defects appear on the surface of Cu metals

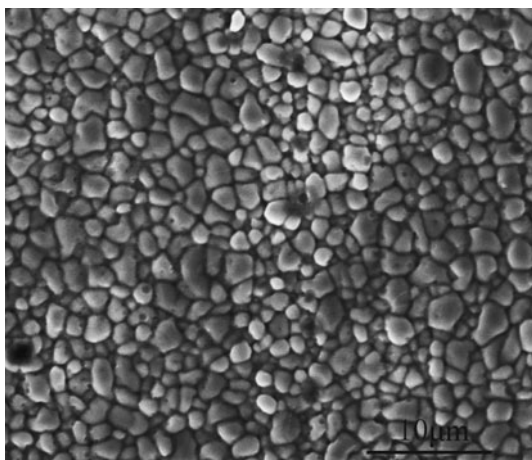


Fig. 7 Morphology of the interfacial intermetallics at Sn-Zn/Cu

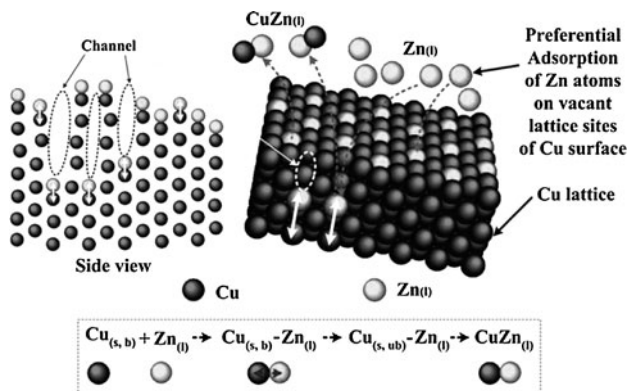


Fig. 8 Schematic diagram of dissolution of Cu in the molten solder

[15]. When soldering, the Zn atoms in the liquid solder are preferential adsorbed to the active defects of Cu foils. As shown in Fig. 8, $Cu_{(s,b)}$ is the Cu atom on the solid Cu lattice, $Zn_{(l)}$ is the Zn atom of the molten solder. The $Zn_{(l)}$ attacks the $Cu_{(s,b)}$, which will reduce bonding strength between the $Cu_{(s,b)}$ and other Cu atoms on the solid Cu lattice. Then the metastable $Cu_{(s,ub)}-Zn_{(l)}$ appears. Subsequently, the $Cu_{(s,ub)}-Zn_{(l)}$ diffuses into the molten solder and forms the $CuZn_{(l)}$. When the temperature decreases to the room temperature, the Cu_5Zn_8 phase is formed.

As shown in Figs. 6 and 9, the thickness of the IMCs formed at the Sn-Zn-xCe/Cu interface increases with the addition of the Ce. When the content of Ce is 0.5 wt%, the thickness of the IMCs is about 13.3 μm, near to 5 times of that of Sn-9Zn/Cu. The standard Gibbs free energy of formation for Sn-Ce compound is much lower than that of the Zn-Sn compound [12]. The addition of Ce makes much more content of Zn diffuse to the interface of solder/Cu to react with Cu substrate because of the “high affinity between Sn and Ce” [11]. So the IMCs become much thicker with the addition of Ce.

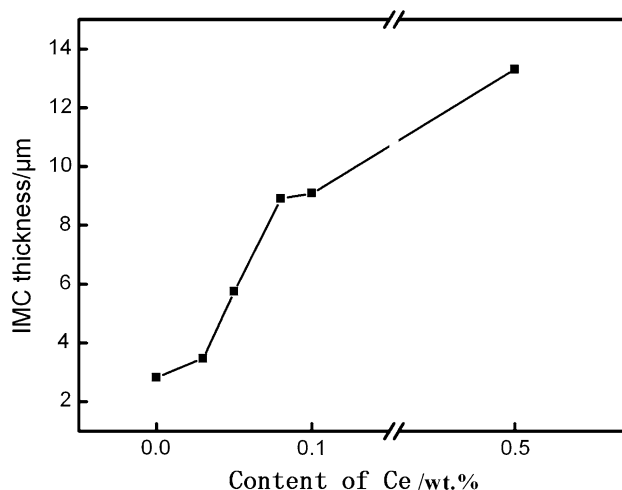


Fig. 9 The IMCs thickness of Sn-9Zn-xCe/Cu

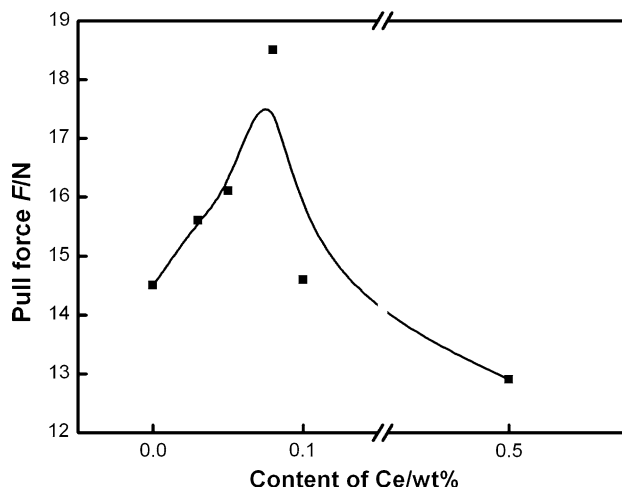


Fig. 10 Strength of the soldered joint

3.4 Mechanical property of soldered joint

The effect of Ce alloying additives on mechanical properties can be seen from Fig. 10. Results show that joint strength is improved by adding appropriate amount of Ce, and the peak value acquired with 0.08 wt% Ce addition, 18.5 N. However, when the content of Ce exceeds 0.1 wt%, joint strength degenerates. When the content of Ce is 0.5 wt%, the pull force is reduced to 12.9 N, even lower than that of Sn-9Zn solder.

The change of mechanical properties by the addition of Ce, can be explained from the fracture morphology of soldered joint, as shown in Fig. 11. Fracture morphology of Sn-9Zn soldered micro-joints shows plenty of dimples, which indicates the fracture type is ductile fracture, since dimples are the typical characteristic of toughness fracture [16], and intense plastic deformation appears before

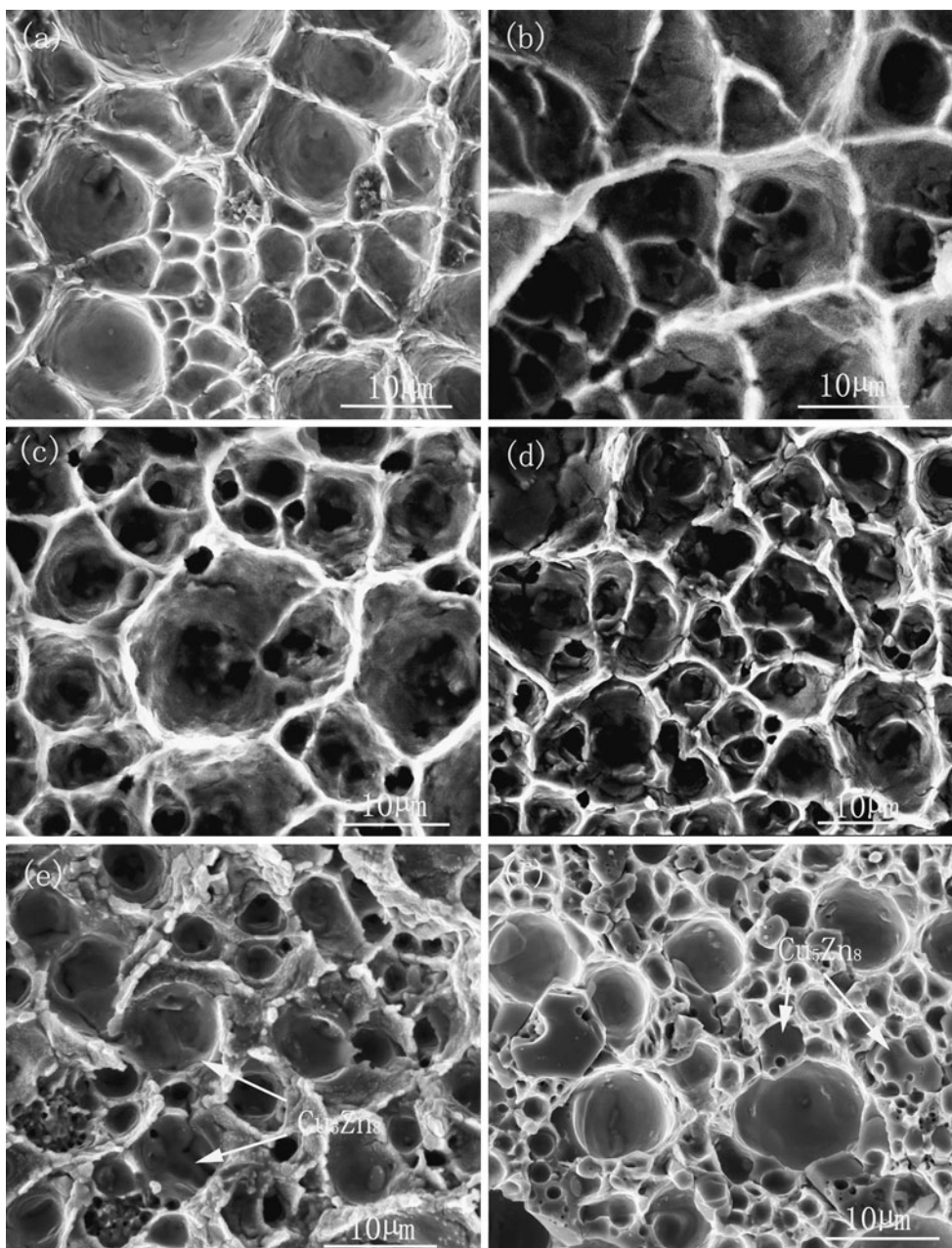


Fig. 11 Fracture morphologies of soldered joints **a** Sn-9Zn, **b** Sn-9Zn-0.03Ce, **c** Sn-9Zn-0.05Ce, **d** Sn-9Zn-0.08Ce, **e** Sn-9Zn-0.1Ce, **f** Sn-9Zn-0.5Ce

fracture. No IMCs are found on the fracture morphology of Sn-9Zn soldered joint, so the fracture occurred in the solder itself. The dimples in the Sn-9Zn-0.08Ce soldered joint are much finer than that in that of Sn-9Zn, which reflects the microstructure refinement by Ce addition. In addition, as shown in Fig. 3d, a uniform and fine structure is obtained. Thus according to the mechanism of grain refinement strengthening, the biggest pull force is obtained when the content of Ce is 0.08 wt% as shown in Fig. 10.

When the Ce content is 0.1–0.5 wt%, some Cu-Zn IMCs appear in the bottom of dimples, as shown in Fig. 10e, g. The IMCs are hard and brittle, and they are easy to be the stress concentration area in the process of soldering, thus IMCs become the source of crack initiation and expansion. According to the section of 3.3, the IMCs become much thicker with the addition of 0.1–0.5 wt% Ce, thus correspondingly, the pull force of Sn-9Zn-(0.1, 0.5)Ce soldered joint decreases, as shown in Fig. 10.

4 Conclusions

- (1) Adding 0.08 w.% Ce to the solder can make Sn–9Zn–xCe alloy form finer microstructure than Sn–9Zn alloy, and some particulate-shaped Sn–Ce compounds appear in the solder when the content of Ce is 0.1–0.5 wt%.
- (2) The wettability of Sn–9Zn solder is significantly improved when the quantity of Ce added in the solder is 0.08 wt% because the surface tension of molten solder is decreased effectively by appropriate addition of Ce.
- (3) In Sn–Zn soldering, a planar Cu₅Zn₈ IMCs layer is formed at Sn–9Zn/Cu interface. The addition of Ce makes much more content of Zn diffuse to the interface of solder/Cu to react with Cu and the IMCs become much thicker than that of Sn–9Zn/Cu.
- (4) The biggest pull force is obtained when the content of Ce is 0.08 wt%. When the Ce content is 0.1–0.5 wt%, some hard and brittle Cu–Zn IMCs appear in the bottom of dimples and the pull force of soldered joint decreases.

Acknowledgement The authors acknowledge the financial support from Jiangsu Six Kind Skilled Personnel Project (No. 06-E-020).

References

1. N.S. Liu, K.L. Lin, Evolution of interfacial morphology of Sn-8.5Zn-0.5Ag-0.1Al-xGa/Cu system during isothermal aging. *J. Alloys Compd.* **456**(1–2), 466–473 (2008)
2. C.F. Yang, F.L. Chen, W. Gierlotka, Thermodynamic properties and phase equilibria of Sn-Bi-Zn ternary alloys. *Mater. Chem. Phys.* **112**, 94–103 (2008)
3. L. Zhang, S.B. Xue, L.L. Gao, G. Zeng, Z. Sheng, Y. Chen, S.L. Yu, Effects of rare earths on properties and microstructures of lead-free solder alloys. *J. Mater. Sci. Mater. Electron.* **20**(8), 685–694 (2009)
4. C.M.L. Wu, C.M.T. Law, D.Q. Yu, L. Wang, The wettability and microstructure of Sn-Zn-RE alloys. *J. Electron. Mater.* **32**(2), 63–69 (2003)
5. C.K. Behera, M. Shamsuddin, Thermodynamic investigations of Sn-Zn-Ga liquid solutions. *Thermochim. Acta* **487**, 18–25 (2009)
6. J. Zhou, Y.S. Sun, F. Xue, Effect of Nd and La on surface tension and wettability of Sn-8Zn-3Bi solders. *Trans. Nonferrous Met. Soc. Chin.* **15**(5), 1161–1165 (2005)
7. X. Chen, A.M. Hu, M. Li, D.L. Mao, Study on the properties of Sn-9Zn-xCr lead-free solder. *J. Alloys Compd.* **460**, 478–484 (2008)
8. T.C. Hsuan, K.L. Lin, Microstructural evolution of ϵ -AgZn₃ and η -Zn phases in Sn-8.5Zn-0.5Ag-0.01Al-0.1 Ga solder during aging treatment. *J. Alloys Compd.* **409**, 350–356 (2009)
9. C.M.L. Wu, D.Q. Yu, C.M.T. Law, L. Wang, Properties of lead-free solder alloys with rare earth element additions. *Mater. Sci. Eng. R Rep.* **44**(1), 1–44 (2004)
10. C.M.L. Wu, Y.W. Wong, Rare-earth additions to lead-free electronic solders. *J. Mater. Sci. Mater. Electron.* **18**(1–3), 77–91 (2007)
11. C.M.L. Wu, D.Q. Yu, C.M.T. Law, L. Wang, The properties of Sn-9Zn lead-free solder alloys doped with trace rare earth elements. *J. Electron. Mater.* **31**, 921–927 (2002)
12. R. Mahmudi, A.R. Geranmayeh, B. Zahiri, M.H. Marvasti, Effect of rare earth element additions on the impression creep of Sn-9Zn solder alloy. *J. Mater. Sci. Mater. Electron.* doi:[10.1007/s10854-009-9870-y](https://doi.org/10.1007/s10854-009-9870-y)
13. J.X. Wang, S.B. Xue, Z.J. Han, S.L. Yu, Y. Chen, Y.P. Shi, H. Wang, Effect of rare earth Ce on microstructures, solderability of Sn–Ag–Cu and Sn–Cu–Ni solders as well as mechanical properties of soldered joints. *J. Alloys Compd.* **467**(1–2), 219–226 (2009)
14. C.M. Chen, C.H. Chen, Interfacial reactions between eutectic SnZn solder and bulk or thin-film Cu substrates. *J. Electron. Mater.* **36**, 1363–1371 (2007)
15. C.H. Yu, *Investigations of the Effect of Element in Sn-Zn-Ag Solder With the Reaction of Cu Metal During Soldering* (National Cheng Kung University, Taiwan, 2006)
16. Z.J. Han, S.B. Xue, J.X. Wang, X. Zhang, L. Zhang, S.L. Yu, H. Wang, Mechanical properties of QFP micro-joints soldered with lead-free solders using diode laser soldering technology. *Trans. Nonferrous Met. Soc. Chin.* **18**, 814–818 (2008)